Pergamon

0301-9322(94)00081-6

Int. J. Multiphase Flow Vol. 21, No. 3, pp. 365–379, 1995

0301-9322/95 $9.50 + 0.00

A STUDY OF TERRAIN-INDUCED SLUGGING IN TWO-PHASE FLOW PIPELINES

V. DE HENAU† and G. D. RAITHBY

Department of Mechanical Engineering, University of Waterloo, Waterloo, Ontario, Canada N2L 3G1

(Received 28 April 1994; in revised form 4 November 1994)

Abstract—The presence of gas and liquid flowing simultaneously in pipelines made of several uphill and downhill sections can lead to the formation of long liquid slugs which are blown from one pipeline section to the next due to gas pressure. This terrain-induced slugging gives rise to undesirable unsteady flow conditions. In this paper, a transient two-fluid model is validated for conditions of terrain-induced slugging. This model contains new correlations, for the drag coefficient and the virtual mass force for the slug flow regime, that were presented in previous papers. An experimental study of terrain-induced slugging in a laboratory scale pipeline, made of two uphill and two downhill sections, is also reported. This provides data for the model validation. The model predicts all the major features of the data, and is in good quantitative agreement as well.

Key Words: gas–liquid flow, two-fluid models, slug flow, terrain-slugging, transient, unstable flow, pipeline, experimental

1. INTRODUCTION

Most offshore pipelines transport natural gas and oil simultaneously. Depending on factors such as the terrain topography and the local flow conditions, the liquid phase can accumulate in the low points of the pipeline, forming long liquid bridges that can be blown out from one pipeline section to the next by the gas pressure. This phenomenon, called terrain-induced slugging, gives rise to large fluctuations in the liquid outflow rate. In order to size the gas–liquid separator at the outlet of the pipeline, a good estimate of the volume of liquid entering the separator is required; such an estimate is difficult to obtain under conditions of terrain-induced slugging.

Much of the work related to terrain-induced slugging is restricted to the study of severe slugging in pipeline–riser systems with a constant separator pressure. Experimental studies of severe slugging in pipeline–riser systems have been conducted, for example, by Schmidt *et al.* (1985) and Fabre *et al.* (1990). Models to predict severe slugging in pipeline–riser systems have been developed by Schmidt *et al.* (1985), Taitel *et al.* (1990a), Fabre *et al.* (1990) and Sarica & Shoham (1991).

Although severe slugging in a pipeline–riser system exhibits a cyclic behaviour similar to the one observed for terrain-induced slugging in undulating pipelines, the analysis of the latter is more complex since upstream and downstream flow conditions affect the blowout process. In an attempt to account for this upstream and downstream influence, Taitel *et al.* (1990b) extended a severe slugging model to handle unstable flow in a pipeline with multiple uphill and downhill sections. This model is valid only for low flow rates of gas and liquid since all dynamic terms and friction losses in the momentum balance have been neglected. Predictions obtained for a hypothetical undulating pipeline displayed the cyclic behaviour in the pressure that is typical of terrain-induced slugging. It is not known, however, if the predicted cycle times are realistic. It is also noted that this model is restricted to terrain-induced slugging and cannot be applied to general transient two-phase flow problems in pipelines.

In recent years, several transient two-fluid models were also developed to simulate transient phenomena in pipelines. Taitel *et al.* (1989), for example, proposed a simplified transient model which assumes a quasi-steady gas flow and a local momentum equilibrium balance. The main limitation of this model with regards to terrain-induced slugging is the assumption that the gas flow

†Present address: GEC ALSTHOM Electromécanique, 1500 rue Vandal, Tracy, Québec, Canada J3R 5K9.

rate is constant at any cross-section of the pipeline. Bendiksen *et al.* (1991) developed a transient two-fluid model, called OLGA, in which the interphase interactions are accounted for through correlations that depend on the flow regime. The model performed well for various steady-state and transient flow problems in pipes. OLGA does not, however, account for the virtual mass force in the slug flow regime, which can result in non-physical oscillations in the predictions (De Henau & Raithby 1995b). It also assumes that the pressure for both phases is equal. This assumption can lead to important instabilities in the solution for the case of stratified flow (Banerjee 1986), which is the dominant flow regime in the downhill portions of a pipeline.

The purpose of the present paper is to validate a transient two-fluid model, developed by De Henau & Raithby (1995a), for cases of terrain-induced slugging in an undulating pipeline. The model uses a standard approach for stratified flow, which accounts for the pressure difference between the gas and the liquid phases (see De Henau 1992). It also uses new correlations for the drag coefficient and the virtual mass force in a slug flow regime. These correlations have been tested with good success for steady and transient slug flows in horizontal and inclined pipes (De Henau & Raithby 1995b). The model being based on basic conservation principles, it is not restricted to terrain-induced slugging and can be used to solve general transient slug flow problems in pipelines.

Because there is a lack of data for terrain-induced slugging in an undulating pipeline, an experimental study using air and water in a laboratory scale pipeline made of two uphill and downhill sections was undertaken to assess the performance of the model.

In the next section, a brief description of the experimental set-up is given. This is followed by a discussion on the experimental results and the comparisons between the data and the model predictions.

2. DESCRIPTION OF THE EXPERIMENTAL APPARATUS

2.1. Experimental layout

A schematic of the experimental layout is shown in figure 1. The test section consists of four sections of smooth transparent PVC pipe, each having an inside diameter of 51.8 mm and a length of 3.84 m. The pipes are connected together with smooth flexible hoses of the same diameter and

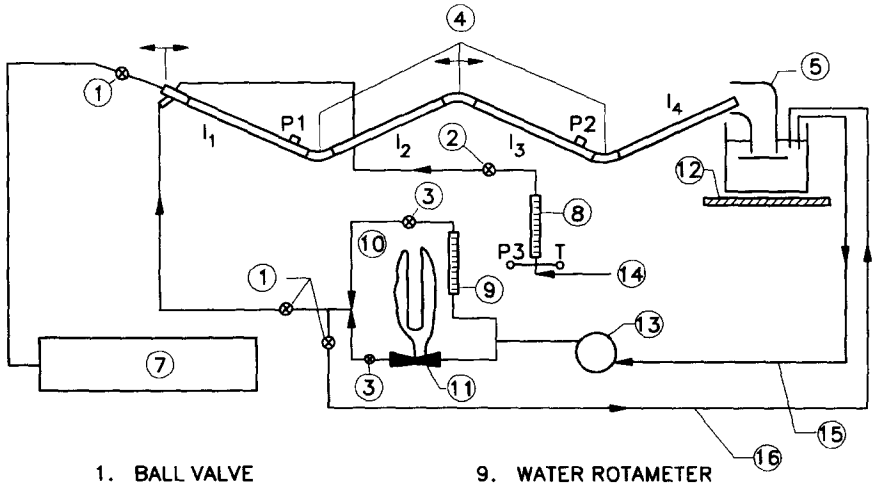

1. BALL VALVE
2. NEEDLE VALVE
3. GATE VALVE
4. FLEXIBLE HOSE
5. DEFLECTOR
6. RESERVOIR
7. PVC TANK
8. AIR ROTAMETER
9. WATER ROTAMETER
10. MANOMETER
11. VENTURI METER
12. LOAD CELL
13. PUMP
14. AIR CIRCUIT
15. WATER PRIMARY CIRCUIT
16. WATER SECONDARY CIRCUIT

Figure 1. Schematic of the experimental apparatus for terrain-induced slugging study.

each having a length of 0.314 m, to form a pipeline with two downhill and two uphill sections. The pipeline is attached to steel angles mounted on a roller system which allows for a range of inclination angles from ± 10 to $\pm 30°$.

The entrance of the pipeline is fitted with a three-way injector, with one inlet for the air flow, one for the water flow and a third inlet which is connected to a large PVC tank. The tank adds a volume that is equivalent to an additional pipeline length of 53 m (for a 51.8 mm diameter) upstream of the first uphill section. The additional volume is necessary to reproduce terrain-induced slugging, as discussed by Taitel *et al.* (1990b). This approach to obtain the additional volume was used by Taitel *et al.* (1990a) in their experiments for severe slugging in a pipeline–riser system.

At the outlet of the pipeline, the air and the water are separated by gravity, the air being vented to the atmosphere and the water being collected in a reservoir to be pumped back into the pipe. The reservoir is installed on a load cell to record the mass variations as water is added to or pumped from the reservoir. A deflector is attached to the outlet to reduce the impulse of the liquid slugs on the water in the reservoir and to attenuate the wave motion at the surface of the water.

2.2. The air and water supply systems

The air is supplied from a central compressed air reservoir at a constant pressure of about 650 kPa. The air flow rate is controlled by a needle valve.

Filtered city tap water is used for the experiments. The water is pumped from the reservoir to the inlet of the pipeline by a centrifugal pump, with a capacity to supply about 65 l/min.

2.3. The instrumentation

The air flow rate is measured by a rotameter equipped either with a glass float or a stainless steel float. The rotameter range is from 0.5 to 70 l/min. The average error on the measured air flow rates is $\pm 2\%$. The maximum error is $\pm 6\%$.

The air pressure and temperature, which are required to calculate the air density, are measured near the inlet of the rotameter. The maximum error in the temperature reading is $\pm 0.1°C$. The estimated error on the pressure is ± 1.5 kPa for a pressure of 650 kPa.

The water flow rate is measured by a rotameter and a venturi meter connected to a U-tube manometer. Both flowmeters can be used independently or in parallel. The estimated error (with a 95% confidence level) for the water flow rate measurements is ± 0.0036 to ± 0.0131 kg/s for a mass flow rate from 0.0315 to 1.090 kg/s, respectively.

The pressures P_1 and P_2 are measured at stations P1 and P2, which are 3.72 and 11.98 m, respectively, from the inlet of the pipeline, using corrosion-resistant gauge pressure transducers. The estimated error (with a 95% confidence level) for the pressure measurements is ± 0.05 to ± 0.16 kPa for a gauge pressure from 0 to 35.0 kPa, respectively.

The mass variation of the water reservoir is recorded by a load cell. The load cell has a maximum load limit of 54 kg with a maximum error of ± 0.0369 kg (with a 95% confidence level).

The data acquisition is done with a PC-LabCard PCL-860, DC/AC voltmeter card with a 16 bit digital output installed in a IBM PC-XT computer. A PCLD-788 Relay Multiplexer Board is connected to the voltmeter to allow the use of four channels (three for the pressure transducers and one for the load cell).

2.4. The experimental procedure

The time variation of the pressures P_1 and P_2, and of the outlet water mass flow rate, Q_L, are required for given inlet flow rates of air and water.

The outlet water mass flow rate Q_L is obtained from a simple mass balance on the water reservoir. It is expressed as:

$$Q_L = \left[\frac{\Delta m}{\Delta t} \right] + \dot{m}_{\text{pump}} \qquad [1]$$

where $[\Delta m/\Delta t]$ is the derivative of the water reservoir mass with respect to time and $\dot{m}_{\text{pump}}$ is the mass flow rate of the pump. To reduce the large oscillations in the measured Q_L which are caused

by the intermittent nature of slug flow, numerical filtering is required. To evaluate $[\Delta m/\Delta t]$ at a time n from the data obtained at times $n-1$, n, $n+1$, the following is used:

$$\left[\frac{\Delta m}{\Delta t}\right]_n = \frac{1}{3}\sum_{k=n-1}^{n+1}\frac{m_{k+1}-m_{k-1}}{t_{k+1}-t_{k-1}} \qquad [2]$$

3. RESULTS AND DISCUSSION

The experiments are classified into two groups: the stable or steady-state cases and the terrain-induced slugging cases. For the stable cases, the pipeline system is isolated from the PVC tank (shown in figure 1) and a steady-state two-phase flow results, with stratified flow in the downward sections and the slug flow in the upward sections. In the terrain-induced slugging cases, the PVC tank is opened to the pipeline system; a cyclic behaviour is observed, during which water fills the uphill sections and part of the downhill sections before being impulsively blown out of the system by the pressurized gas.

Numerical predictions of the stable and terrain-induced slugging cases are obtained using the transient two-fluid model for slug flow which is described in the papers of De Henau & Raithby (1995a,b). The other flow regimes which are incorporated into the two-fluid model (i.e. stratified, annular and bubbly flows) are adopted from standard models and are described in De Henau's work (1992). The unified flow regime transition model of Barnea (1986, 1987) is used in the transient model with some small modifications to account for the transient effects (see De Henau 1992).

3.1. The stable cases

3.1.1. Description of the experimental results. Experiments are conducted with two different sets of inclination angles θ_1, θ_2, θ_3 and θ_4, for sections l_1, l_2, l_3 and l_4, respectively, illustrated in figure 2. The angles, taken with respect to the horizontal, are listed in table 1.

Although experimental and numerical results for stable cases were obtained for a wide range of inlet flow rates, only two cases are presented in this paper. The inlet superficial velocities for the gas phase, $u_{Gs,0}$ (based on a temperature of 21°C and a pressure of 101,325 Pa), and for the liquid phase, u_{Ls}, as well as the ambient temperature T and the atmospheric pressure P_0 for those cases, are given in table 2.

Figure 3 illustrates typical experimental measurements (dotted lines) for the time evolution of the pressure P and outlet water mass flow rate Q_L for a stable case with $u_{Ls} = 0.1275$ m/s and $u_{Gs,0} = 0.1283$ m/s and the angles from set 1. The pressure ratio P/P_0 represents the ratio of the absolute pressure P_1 or P_2 to the atmospheric pressure for the given experiment.

To understand the experimental results in figure 3, it is necessary to envisage the development of the flow. As soon as the water is injected in the pipeline system, it flows down section l_1 as a stratified layer and starts to fill up section l_2 (see figure 2). The air–water interface in l_1 (I_1) is located at the bottom of that section, allowing gas to flow through the water in section l_2. The fact that the interface I_1 stays at the bottom of l_1 indicates that the pressure differences (this difference being $P_1 - P_0$, since P at I_2 is about P_0) and the drag force by the air on the water in l_2 are in balance with the weight of the water.

Water therefore fills l_2 while gas flows through it, giving rise to a slug flow regime in the first uphill section. At the same time, the pressure P_1 increases due to the increasing weight of liquid in l_2; this rise is labelled A_1 in figure 3. The plateau B_1 observed in P_1 (at $t \approx 30$ s) in figure 3 occurs

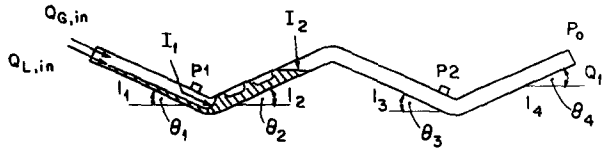

Figure 2. I_1 at bottom of l_1 as gas and water flow in l_2.

Table 1. Inclination angles used in the two-phase flow experimental study

Angle	Set 1	Set 2
θ_1	−15.0°	−25.7°
θ_2	+15.0°	+25.7°
θ_3	−15.0°	−25.4°
θ_4	+13.6°	+24.1°

Table 2. Experimental conditions for stable cases

Run No.	$u_{Gs,0}$ (m/s)	u_{Ls} (m/s)	T (°C)	P_0 (Pa)	Angles Set 1	Angles Set 2
1	0.1283	0.1275	22.4	97826	X	
2	0.4799	0.0668	22.4	97657		X

when the air–water interface in l_2 (I_2 shown in figure 2) reaches the top of that section and water starts to flow down l_3. This plateau results from the fact that there is no net addition of water in section l_2 and the pressure at the top of l_2 remains at P_0 until the water level in l_4 starts to build up. A similar behaviour to the one observed in l_1 and l_2 then occurs in l_3 and l_4, with the air–water interface at the bottom of section l_3 and water filling l_4 under a slug flow regime. The pressure P_2 now rises due to the increase of the weight of water in l_4 (section A_2 in figure 3). The rise in P_1 (denoted by C_1 in figure 3) is a consequence of the rise in P_2. The pressures reach a new plateau as soon as water begins to flow out of the pipeline system. This can be seen in figure 3 by comparing the time at which the pressures level off to the time at which water starts to flow out of the pipeline. At that instant, a stable steady two-phase flow results, with stratified flow in the downhill section and slug flow in the uphill section.

The outlet water mass flow rate Q_L oscillates around the value of the inlet mass flow rate (shown by the straight dash line in figure 3). The oscillations in Q_L are caused by the intermittent nature of the slug flow regime.

For all the stable cases, the trends in the time evolution of the pressures and outlet water mass flow rate are essentially similar to the ones illustrated in figure 3.

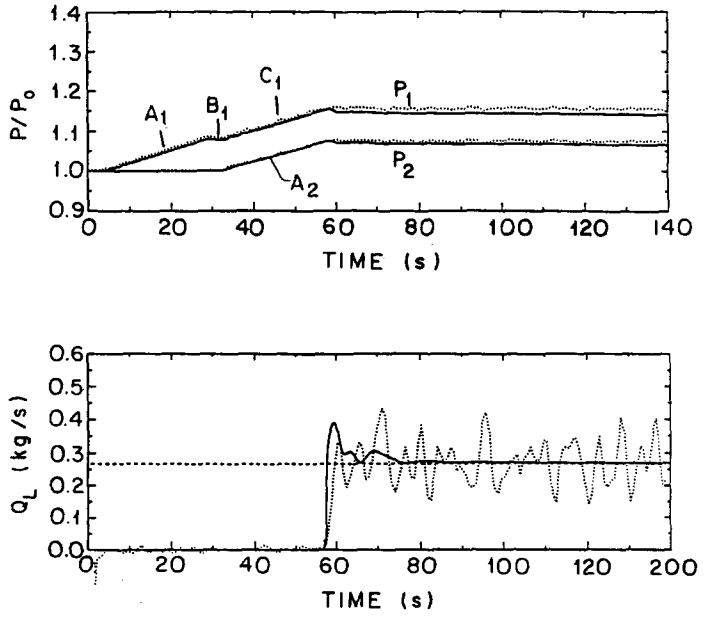

Figure 3. Comparison between experimental data and predictions for time evolution of pressure and outlet water mass flow rate, stable case. Run 1: $u_{Gs,0} = 0.1283$ m/s; $u_{Ls} = 0.1275$ m/s; angles from set 1. ···, experimental data; ——, predictions; – – –, inlet water mass flow rate.

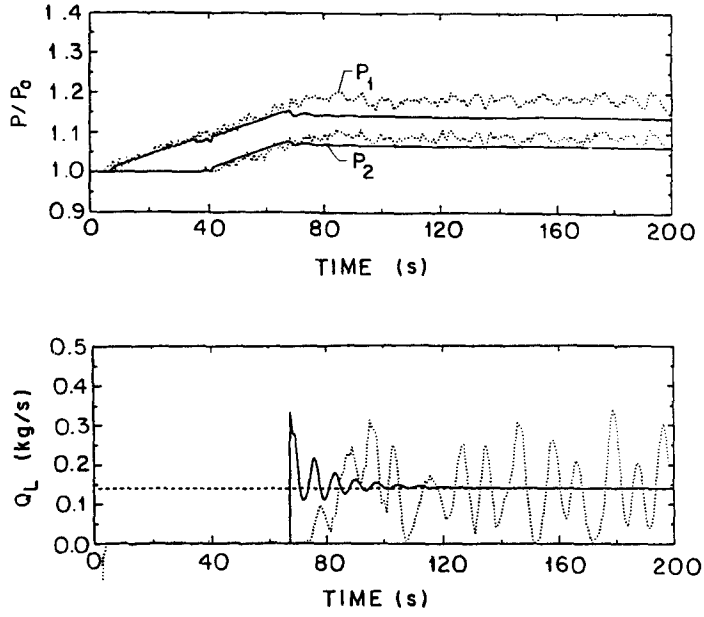

Figure 4. Comparison between experimental data and predictions for time evolution of pressure and outlet water mass flow rate, stable case. Run 2: $u_{Gs,0} = 0.4799$ m/s; $u_{Ls} = 0.0668$ m/s; angles from set 2. ···, experimental data; ——, predictions; – – –, inlet water mass flow rate.

3.1.2. Comparisons between the experimental results and the model predictions. The comparisons between the experimental results and the two-fluid model predictions for the time evolution of the pressure P and outlet water mass flow rate Q_L, for the two stable cases listed in table 2, are shown in figures 3 and 4.

The water and the air properties used in the numerical simulations are given by: water density $\rho_L = 998.2\ \text{kg/m}^3$, water viscosity $\eta_L = 9.930 \times 10^{-4}\ \text{Ns/m}^2$, air viscosity $\eta_G = 1.824 \times 10^{-5}\ \text{Ns/m}^2$, surface tension $\sigma = 0.073$ N/m. The numerical predictions are obtained with a grid size $\Delta x_j = 0.239$ m and a time step $\Delta t = 0.1$ s.

Generally, the best agreement between the computed results and the experimental data is obtained for the lower gas rates, as for the case of run 1 shown in figure 3. The pressure variation with time is very well predicted, with the plateau in P_1 observed when the water starts to flow from section l_2 into section l_3, properly reproduced by the model. The time at which the pressures become constant is also very well predicted for those cases, which is in agreement with the comparisons between the computed and measured time at which the water starts to flow out of the pipeline.

For a high air flow rate, the predicted steady-state pressure levels are lower than the measured ones, as shown in figure 4 for run 2. It is believed that the lower predicted pressures result from an underestimation of the liquid fractions in the uphill sections of the pipeline. The same discrepancy is observed when comparing the two-fluid model computations for the liquid fraction and the pressure drop to experimental data for steady-state air–oil slug flow in inclined pipes (see De Henau & Raithby 1995b). It is noted that the correlation to calculate the slug unit translational velocity v_t has a strong influence on the liquid fraction level (through the drag coefficient between the phases) and, therefore, on the magnitude of the computed pressure gradients. This influence is the same for steady or transient slug flow. The correlation for v_t of Théron (1989), which is used in the present predictions, is dependent on a drift velocity that varies with the inclination angle of the pipes. This correlation was however developed based on data for horizontal air–water slug flow and may not be as accurate for inclined slug flows.

In the case of run 2 (figure 4), the model also predicts that the water flows out of the pipeline at an earlier time than in the experiment. This also indicates that the predicted amount of water that remains in the pipeline is too small, consistent with the underprediction of pressures.

It is noted in figures 3 and 4 that the oscillations in the measured outlet water mass flow rate are not reproduced by the model. Because the present model treats that regime by averaging the

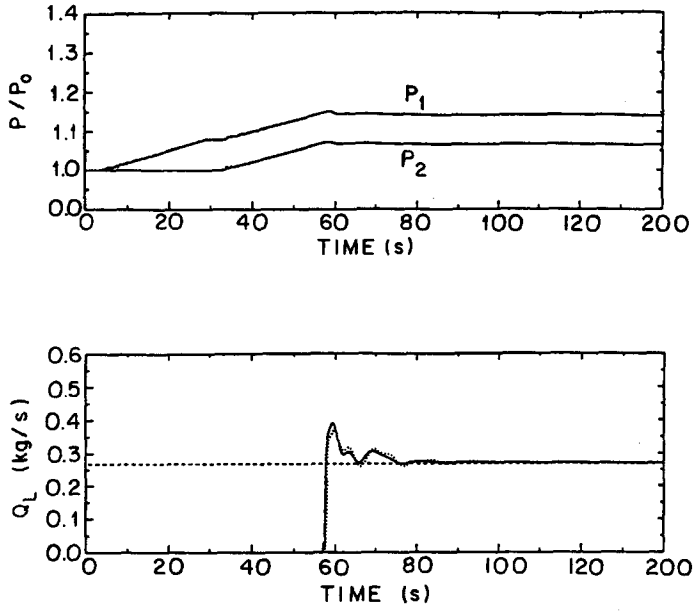

Figure 5. Grid size and time step effects on time evolution of pressure and outlet water mass flow rate, stable case. Run 1: $u_{Gs,0} = 0.1283$ m/s; $u_{Ls} = 0.1275$ m/s; $\Delta x_j/\Delta t = 2.39$ m/s; angles from set 1. ···, $\Delta x_j = 0.120$ m; ——, $\Delta x_j = 0.239$ m; – – –, inlet water mass flow rate.

velocities and liquid fractions in a slug unit over computation control volumes, such oscillations are filtered out. The computed steady-state outlet mass flow rates coincide with the inlet flow rates, as they must for a steady flow.

3.1.3. Grid size and time step sensitivity analysis. The results presented in figures 3 and 4 were computed with a fine enough spatial grid, and a small enough time step, that the predictions are nearly grid independent. This section presents a few of the results that were used in reaching this conclusion. Only the results for run 1 are presented here as the same conclusions are drawn from all the test cases. A constant ratio $\Delta x_j/\Delta t = 2.39$ m/s is chosen, with Δx_j values of 0.120, 0.239 and 0.478 m for the straight sections of the pipeline. The grid sizes for the curved sections of the pipeline are slightly different, these being 0.105, 0.209 and 0.314 m, respectively.

The predictions shown in figure 3, which were obtained with $\Delta x_j = 0.239$ m, are reproduced as the solid curves in figure 5, and are compared to the predictions for the 0.120 m grid. This figure shows that there is only a small effect of the grid size on the predictions. The other test for $\Delta x_j = 0.478$ m gives virtually the same pressure distributions as the finer grids with, however, a slight delay in the time at which water starts to flow out of the pipeline.

3.2. The terrain-induced slugging cases

3.2.1. Description of the experimental results. For the terrain-induced slugging cases, the PVC tank is opened to the pipeline system; the additional volume provided by the tank is necessary to

Table 3. Experimental conditions for terrain-induced slugging cases

Run No.	$u_{Gs,0}$ (m/s)	u_{Ls} (m/s)	T (°C)	P_0 (Pa)	Angles	
					Set 1	Set 2
3	0.0625	0.1230	21.2	97590	X	
4	0.1249	0.1197	22.2	97657	X	
5	0.1254	0.3377	22.2	97623	X	
6	0.4801	0.0551	22.9	96982	X	
7	0.4827	0.1406	22.8	97049	X	
8	0.0616	0.0545	20.4	98467		X
9	0.1244	0.1287	22.7	98130		X
10	0.1248	0.2387	21.4	99143		X
11	0.2519	0.0516	20.6	97252		X

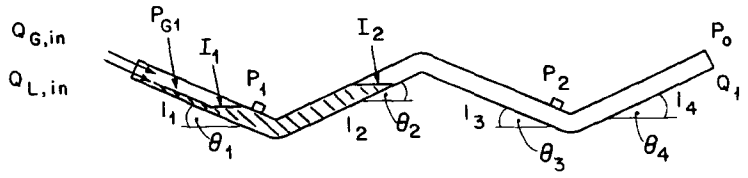

Figure 6. Water level rising in l_1 and l_2.

obtain terrain-induced slugging in the pipeline system used in this experimental study. Only air can flow in and out of the tank. The same set of inclination angles as for the stable cases are used in the experiments for terrain-induced slugging (see table 1).

The superficial liquid velocity ranges from about $u_{Ls} = 0.05$ to 0.35 m/s. The maximum liquid superficial velocity is limited to avoid water from flowing back into the PVC tank. For the air, the superficial velocity, based on a temperature of 21°C and a pressure of 101,325 Pa, is varied from $u_{Gs,0} = 0.06$ to 0.50 m/s. The experimental flow conditions for the unstable cases presented in this paper are listed in table 3.

Using the schematic drawings in figures 6 and 7, the pressure and water outflow distributions in figure 8 are described. The conditions correspond to run 9 in table 3. As for the stable cases, the pressure P_1 increases linearly along A_1 in figure 8 for the conditions shown in figure 6. Note however that the large inlet volume (PVC tank plus section l_1) causes the gas pressure P_{G1} to increase more slowly so that the interface I_1 moves back up in section l_1. This also causes the pressure P_1 to be higher than P_{G1}, preventing gas from moving through section l_2. The plateau B_1 occurs when the liquid first overflows from l_2 into l_3. The steady rise in P_1 and P_2 occurs as soon as the elbow between l_3 and l_4 fills with liquid, trapping air in l_3. As liquid continues to flow into l_3, the liquid rises in l_4 which, by its hydrostatic pressure, compresses the gas in l_3 and causes I_3 to move backwards up section l_3. At the point where liquid first leaves l_4, Q_L suddenly increases and both P_1 and P_2 become constant, as shown in figure 8. The flow pattern at this point appears in figure 7.

As liquid and gas continue to flow into l_1, the pressure P_{G1} gradually increases, causing I_1 to move slowly down l_1. The pressure P_1 and P_2 remain constant, as indicated by D_1 and D_2 in figure 8. At the instant the interface I_1 reaches the bottom of l_1, air penetrates the water in l_2, displacing some of the water from that section. This results in a decrease in the pressure P_{G1} that is needed to maintain a force balance on the liquid in section l_2. The escape of gas from l_1 does indeed drop the pressure P_{G1}, but because of the large volume for the gas phase, it drops at a lower rate than required to just balance the forces. A net force is therefore present across l_2 that accelerates the liquid–gas mixture downstream. As more liquid is forced out of l_2, the force imbalance increases and a blowout is underway. The sudden air and water flow into l_3 triggers a blowout of the water in l_4. During the blowout process, the pressures P_1 and P_2 drop sharply as the liquid exits the pipeline (see figure 8 for $t \approx 143$ s). The outlet water mass flow rate increases rapidly, but drops to zero once the blowout is completed. The cycle then repeats itself. During a blowout, a highly aerated slug flow regime is formed in the uphill section, with slug units having very irregular shapes and moving at high velocities.

As can be seen in figure 8, all the cycles following the first blowout have the same period which is shorter than the one for the initial cycle. This is explained partly by the presence of a liquid residual that remains in the low points of the pipeline after a blowout, reducing the time required to fill the uphill sections. Another reason is the temperature fluctuations in the PVC tank. During

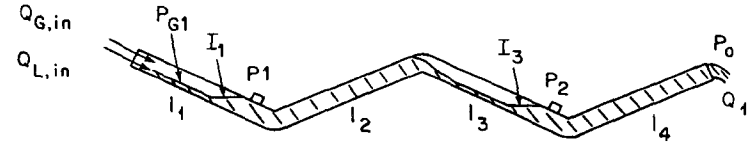

Figure 7. Water and air distribution as water starts to exit the pipeline prior to a liquid blowout.

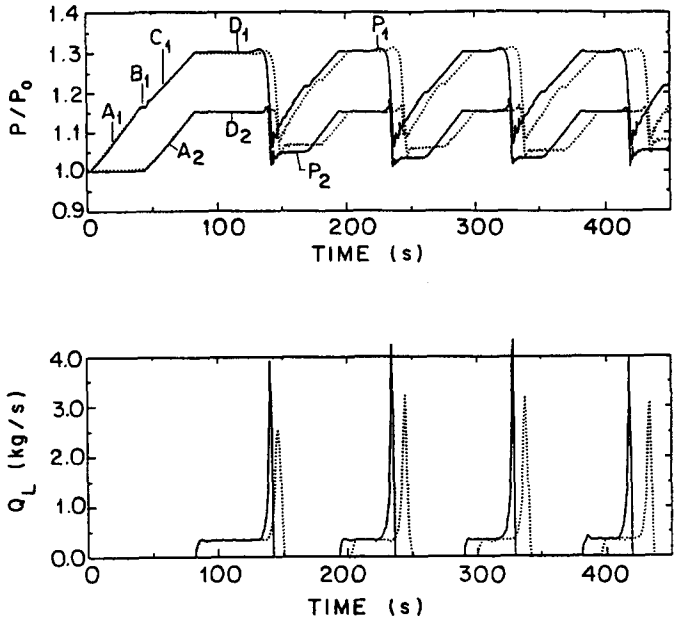

Figure 8. Comparison between experimental data and predictions for time evolution of pressure and outlet water mass flow rate, terrain-induced slugging type I. Run 9: $u_{Gs,0} = 0.1244$ m/s; $u_{Ls} = 0.1287$ m/s; angles from set 2. · · ·, experimental data; ——, predictions.

a blowout, the temperature drops rapidly as the gas exits the tank. After the blowout, the temperature increases due to heat transfer from the wall of the tank to the air. This temperature rise causes P_{G1} to increase more rapidly than for an isothermal situation, reducing the time for P_{G1} to be high enough to trigger another blowout.

In the present work, all the terrain-induced slugging cases for which there is a time span between the moment water starts to flow out of the pipeline and the moment the blowout occurs (time during which the pressures P_1 and P_2 and the water flow rate Q_L remain constant, as for run 9 in figure 8) are denoted as type I terrain-induced slugging.

Figure 9 shows pressure and flow rate measurements for run 4 which have quite different characteristics; the periods in which P_1, P_2 and Q_L are all constant are missing. This is defined as type II terrain-induced slugging.

In the case of run 4, the inclination angles are smaller so the gravitational force resulting from the weight of water in the uphill sections does not play as dominant a role in the momentum balance as it does with steeper angles. As water fills section l_2 for example, the gas pressure P_{G1} is just high enough to keep the air–water interface I_1 close to the intersection of l_1 and l_2, blocking off completely the passage for the gas flow. The same behaviour is also observed in sections l_3 and l_4. As soon as water starts to exit the pipeline, the interface I_1 is pushed into l_2, allowing gas to penetrate the water. As for run 9, there is a net increase in the force acting on the water in l_2, creating a blowout. This increase is, however, diminished due to the smaller influence from the gravitational force. The intensity of the blowout is also reduced, leaving more water in the pipeline after each cycle. For high inclination angle cases, a type II blowout would result with a high enough gas flow rate. The intensity of the blowout would, however, be greater than for the lower inclination angles.

Hence, the main difference between terrain-induced slugging of type I (figure 8) and of type II (figure 9) is the position of the interfaces I_1 and I_3 (shown in figure 7) as water starts to flow out of the pipeline prior to a blowout. The terrain-induced slugging of type II is more unstable than the type I as small fluctuations in the gas pressure P_{G1} or in the position of I_1 can trigger a blowout. The relative magnitude of the net pressure force acting on the water in an uphill section of the pipeline to that of the gravitational force resulting from the weight of water in that section is the factor that determines which type of terrain-induced slugging prevails.

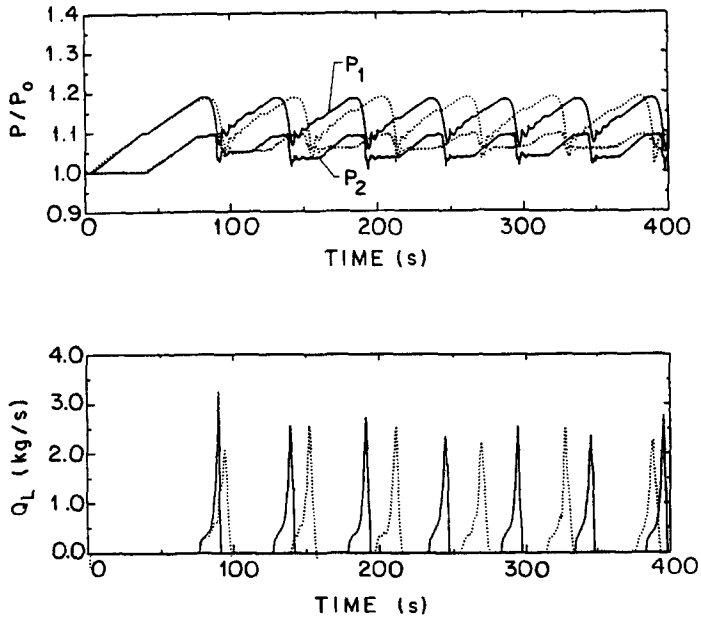

Figure 9. Comparison between experimental data and predictions for time evolution of pressure and outlet water mass flow rate, terrain-induced slugging type II. Run 4: $u_{Gs,0} = 0.1249$ m/s; $u_{Ls} = 0.1197$ m/s; angles from set 1. · · ·, experimental data; ——, predictions.

3.2.2. Special modelling considerations for the terrain-induced slugging cases. The two-fluid model used to compute the terrain-induced slugging problems is the same as the one for the stable cases. A special treatment is required, however, to account for the head loss associated with air flow in the PVC tank through the connecting hoses. In addition, the model being an isothermal model (see De Henau & Raithby 1995a), a thermal energy equation is included to calculate the air temperature variations in the PVC tank. The heat transfer coefficient between the wall of the tank and the air inside the tank is evaluated using standard analysis methods for natural and forced convection in a cylinder (the tank is cylindrical). Details of that analysis and of the derivation of the head loss

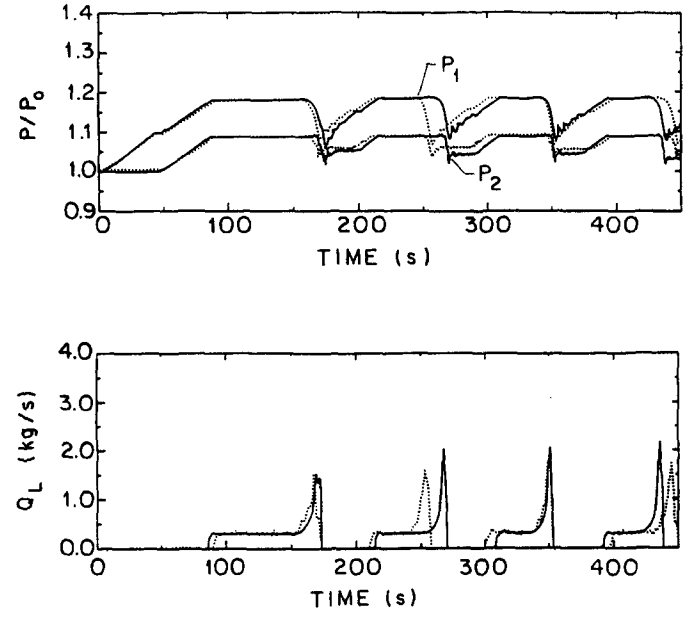

Figure 10. Comparison between experimental data and predictions for time evolution of pressure and outlet water mass flow rate, terrain-induced slugging type I. Run 3: $u_{Gs,0} = 0.0625$ m/s; $u_{Ls} = 0.1230$ m/s; angles from set 1. · · ·, experimental data; ——, predictions.

model are given in the thesis of De Henau (1992). The non-isothermal treatment of the tank is made necessary because of its small surface area to volume ratio which decreases the rate at which the temperature of the air inside the tank rises back to ambient temperature after a blowout. For the pipe itself, the isothermal approximation is reasonable because of the large surface area to volume ratio. No temperature measurements were taken during the experiments but calculations indicated temperature fluctuations inside the tank of the order of 20 K. Treating the compression and expansion in the tank as isothermal resulted in large errors in the predictions of the cycle times for the blowouts.

The influence of transients on the flow regime transition boundaries also needs special consideration. For the transition between stratified (or annular) flow and slug flow, transient effects are already accounted for because the liquid level used in the transition criteria is obtained from the transient solution for the stratified (or annular) flow regime and not from the fully developed steady-state solution as used by Barnea (1986,1987). For the transition from slug to non-slug flow during a blowout however, a particular treatment is required. As an uphill section is being emptied of water during a blowout, the average liquid fraction along the section eventually reaches a level which is too low to sustain a slug flow, causing a transition to stratified or annular flow. This level of the liquid fraction, designated by $h_{L,min}$, is strongly affected by the violence of the blowout and should be a function of the inclination angle of the pipe and of the gas and liquid flow rates. Flow regime transition models, like those proposed by Barnea (1986, 1987) do not account for the influence of transients of the transition boundaries and fail to give a correct value for $h_{L,min}$.

In the present work, the value for $h_{L,min}$ is estimated from the measured P_2 immediately after a blowout. It is assumed that, before falling back to accumulate at the bottom of an uphill section after a blowout, the liquid is uniformly distributed along the section. The liquid fraction of the uniform layer is taken as being the liquid fraction at which transition from slug to stratified or annular flow takes place. $h_{L,min}$ is therefore evaluated as:

$$h_{L,min} = \frac{P_2 - P_0}{\rho_L g l_4 \sin \theta_4} \qquad [3]$$

where P_0 is the atmospheric pressure during the experiments and g is the gravitational acceleration. Taking an average over all the experiments, a value of $h_{L,min}$ greater than 0.5 is obtained for the experiments with the angles from set 1 while a value of 0.38 is estimated for the experiments with the angles from set 2. These values were used in the model as the transition criterion. The value of 0.5 was selected because it represents the upper limit of liquid holdup above which stratified or annular flow are not observed (Dukler & Taitel 1986).

Using this approach to obtain the transition from slug to non-slug flow during a blowout is very approximate but, at the present time, there is no model to predict this transition under transient flow conditions. Except for the selected values of $h_{L,min}$, the present two-fluid model has not been tuned in any way to fit the experimental data.

3.2.3. Comparisons between the experimental results and the model predictions. Figures 8 to 11 compare the experimental data and the two-fluid model predictions for the time evolution of the pressure P and outlet water mass flow rate Q_L, for the terrain-induced slugging cases with various inlet mass flow rates of the gas and liquid phases and various inclination angles. Results for type I terrain-induced slugging are shown in figures 8 (run 9) and 10 (run 3) and for type II in figures 9 (run 4) and 11 (run 6). The numerical predictions are obtained with the same fluid properties, grid size and time step as given in section 3.1.2.

Good agreement between the data and the computations is obtained for the terrain-induced slugging cases of type I. The evolution in time of the pressures P_1 and P_2 and of the outlet water mass flow is well predicted with all the trends in the experiments well reproduced in the computations. It is noticed however that the calculated P_2 levels, right after a blowout, are slightly lower than the measured values, indicating that the model underpredicts the amount of water left in the pipeline after a blowout.

The predicted average cycle times for runs 9 and 3 (figures 8 and 10), as well as for some additional cases of type I, are compared to the experimental times in table 4. The agreement is seen to be excellent.

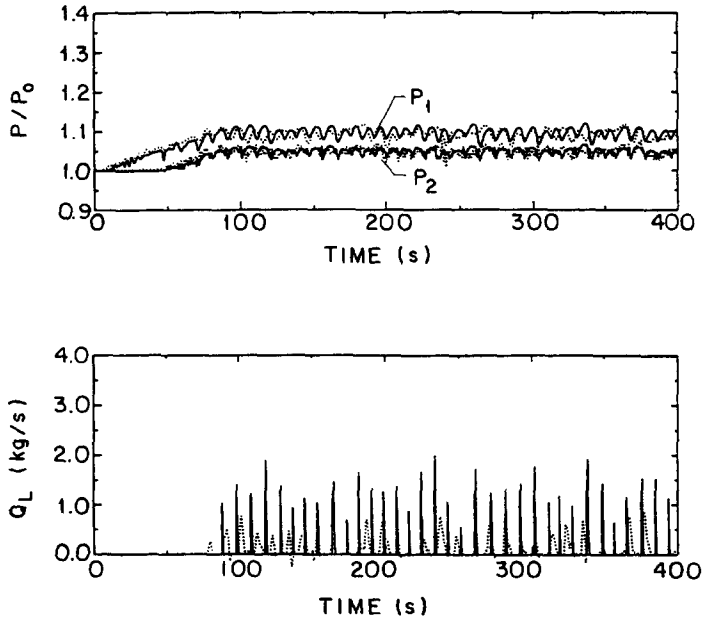

Figure 11. Comparison between experimental data and predictions for time evolution of pressure and outlet water mass flow rate, terrain-induced slugging type II. Run 6: $u_{Gs,0} = 0.4801$ m/s; $u_{Ls} = 0.0551$ m/s; angles from set 1. · · ·, experimental data; ——, predictions.

Figures 9 and 11 show results for low and high gas flow rates for angles from set 1, in which terrain-induced slugging of type II prevails. For those problems, the trends for the time evolution of the pressure and outlet water mass flow rate are generally well predicted by the model. Even the oscillations and kinks in the P_1 and P_2 curves are well reproduced. However, some of the computed cycle times are somewhat in error (see table 4) and the accumulation of cycle time errors cause a displacement in the predictions that makes the results appear worse than they are.

For the type II terrain-induced slugging cases, precise predictions of the cycle time are difficult to obtain because the blowout is very sensitive to small displacements of the air–water interface I_1 at the bottom of section l_1. Parameters that affect the position of I_1 are, for example, the gas pressure P_{G1} (in the tank and in section l_1) and the amount of water left in the pipeline after a blowout. Small errors in the predictions of those parameters strongly influence the cycle time for the blowouts. Because P_{G1} depends on the air temperature in the PVC tank, it is possible in the present numerical study, that the predicted rate of change of P_{G1} is not correct due to uncertainties in the heat transfer modelling for the tank. The upstream difference scheme (UDS) approximations used in the discretization of the advection terms in the momentun equations also introduce errors in the computation of the position of I_1 through the smearing of the interface, which in turn affects the blowout cycles.

The amount of water left in the pipeline after each cycle is strongly related to the drag force acting on the water during a blowout. As mentioned in a previous section, a highly aerated slug flow

Table 4. Comparisons between the experimental and the predicted average cycle times for terrain-induced slugging cases

Run No.	Type I	Type II	Cycle time experimental (s)	Cycle time predicted (s)	% Error
3	X		92.4	87.4	−5.41
4		X	57.9	51.7	−10.7
5	X		45.2	45.0	−0.44
6		X	—	9.2	—
7		X	12.0	11.6	−3.33
8	X		182.5	180.9	−0.88
9	X		95.2	93.0	−2.31
10	X		89.2	89.8	+0.67
11		X	75.2	50.3	−33.12

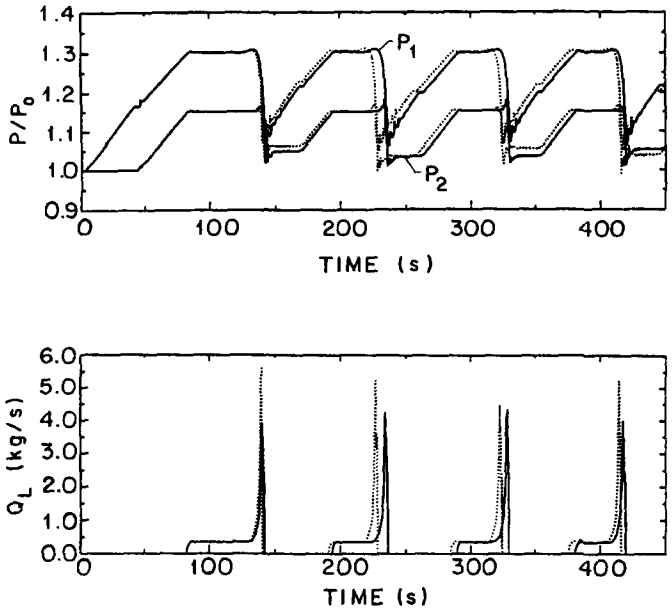

Figure 12. Grid size and time step effects on time evolution of pressure and outlet water mass flow rate, terrain-induced slugging type I. Run 9: $u_{Gs,0} = 0.1244$ m/s; $u_{Ls} = 0.1287$ m/s; $\Delta x_j/\Delta t = 2.39$ m/s; angles from set 2. · · ·, $\Delta x_j = 0.120$ m; ——, $\Delta x_j = 0.239$ m.

regime is formed in the uphill sections of the pipeline during a blowout, with slug units having very irregular shapes and moving at high velocities. Questions arise as to the validity, under those flow conditions, of the assumptions or the correlations used in the slug flow model from which the drag coefficient is estimated. It may well be, for example, that the drag coefficient during a blowout is overestimated, resulting in more liquid being pulled out of the pipeline by the gas phase. It is very difficult, however, to assess the validity of the assumptions and correlations for such cases without more detailed flow measurements.

Although some aspects of the model still need to be refined, the comparisons between the model predictions and the experimental data for the terrain-induced slugging cases show that the model has a great potential for the prediction of such flows.

3.2.4. Grid size and time step sensitivity analysis. The selection of the grid size has an effect on the prediction of the position of the interface at a given time because of the smearing effect resulting from the UDS approximations, as already observed. Experimental observations reveal that a blowout occurs as soon as the air–water interface in a downhill section reaches the intersection of the downhill and uphill sections, allowing gas to penetrate the liquid in the uphill section. If the interface is spread over several control volumes, the gas phase may reach the intersection too soon, precipitating a blowout and therefore reducing the period of each cycle.

The predictions for the time evolution of the pressure P and outlet water mass flow rate Q_L for run 9 (type I terrain-induced slugging), obtained with a grid size of 0.239 m are compared to the predictions with the 0.120 m grid in figure 12. A constant ratio $\Delta x_j/\Delta t = 2.39$ m/s is used in both cases. Although a small effect of grid size and time step is observed, the solutions with $\Delta x_j = 0.120$ m and $\Delta x_j = 0.239$ m are very close to each other with a predicted average cycle period of 91.6 and 93.0 s, respectively. Calculations done with a grid size of 0.478 m (with $\Delta x_j/\Delta t = 2.39$ m/s) gave an average cycle period of 86.7 s. The shorter cycle period for this grid is caused by the smearing of the air–water interface in the downhill sections, as discussed above.

4. CONCLUSIONS

This paper presents the results of an experimental study of terrain-induced slugging in a two-phase flow pipeline, and comparisons between the experimental data and the predictions obtained from a transient two-phase flow model.

In the experimental study, measurements for the pressure and the outlet water mass flow rate are taken for stable or steady-state cases and for terrain-induced slugging cases. In the stable cases, there is an initial transient period during which water fills up the uphill sections; a steady-state two-phase flow is then obtained once water starts to flow out of the pipeline, with stratified flow in the downhill sections and slug flow in the uphill sections. The terrain-induced slugging cases exhibit a cyclic behaviour during which water fills up the uphill sections and the lower portion of the downhill sections to be eventually blown out of the pipeline system. Two types of terrain-induced slugging are observed in the present experimental work, depending on the position of the air–water interface in the downhill sections of the pipeline when water starts to flow out of the pipeline prior to a blowout. The type I is for cases where the interface is not close to the bottom of the downhill sections while in type II, the interface is located near the intersection of the downhill and the uphill sections. The terrain-induced slugging cycle for type II is more sensitive to small displacements of the interface than for type I.

For the stable cases, the model predictions for the time evolution of the pressure and outlet water mass flow rate compare generally very well with the data with some discrepancies due to the correlations used in the slug flow model. For the terrain-induced slugging cases, the model predictions for the time evolution of the pressure and outlet water mass flow rate compare well with the data for type I. In the case of type II, the trends in the measurements are well reproduced by the model but the cycle times are not as well predicted. Because for the type II terrain-induced slugging the blowout cycle is very sensitive to small displacement of the air–water near the intersection of a downhill and uphill section, small errors in the predictions of the parameters which control the position of that interface have an important effect on the computed cycle times.

For both type I and type II, the amount of water left in the pipeline after a blowout is generally underestimated by the model. This is probably due to a poor estimate of the drag coefficient for the slug flow regime in the uphill sections during the blowout.

Although some aspects of the model need to be improved, the results of this research show the potential of the present approach to predict terrain-induced slugging in pipelines.

REFERENCES

BANERJEE, S. 1986 Multifield methods for nuclear thermalhydraulics problems. In *Second International Conference on Simulation Methods in Nuclear Engineering*, Montreal, Canada.

BARNEA, D. 1986 Transition from annular flow and from dispersed bubble flow-unified models for the whole range of pipe inclinations. *Int. J. Multiphase Flow* **12,** 733–744.

BARNEA, D. 1987 A unified model for predicting flow-pattern transitions for the whole range of pipe inclinations. *Int. J. Multiphase Flow* **13,** 1–12.

BENDIKSEN, K. H., MALNES, D., MOE, R. & NULAND, S. 1991 The dynamic two-fluid model OLGA: theory and application. *SPE Prod. Engng* 171–180.

DE HENAU, V. 1992 A study of terrain-induced slugging in two-phase flow pipelines. Ph.D. thesis, University of Waterloo, Waterloo, Ontario, Canada.

DE HENAU, V. & RAITHBY, G.D. 1995a A transient two-fluid model for the simulation of slug flow in pipelines—I. Theory. *Int. J. Multiphase Flow* **21,** 335–349.

DE HENAU, V. & RAITHBY, G.D. 1995b A transient two-fluid model for the simulation of slug flow in pipelines—II. Validation. *Int. J. Multiphase Flow* **21,** 351–363.

DUKLER, A. E. & TAITEL, Y. 1986 Flow pattern transitions in gas–liquid systems: measurement and modelling. In *Multiphase Science and Technology* (Edited by HEWITT, G. F., DELHAYE, J. M. & ZUBER, N.), Vol. 2, p. 1. Hemisphere/Springer, New York.

FABRE, J., PERESSON, L. L., CORTEVILLE, J., ODELLO, R. & BOURGEOIS, T. 1990 Severe slugging in pipeline/riser systems. *SPE Prod. Engng* 299–305.

SARICA, C. & SHOHAM, O. 1991 A simplified transient model for pipeline–riser systems. *Chem. Engng Sci.* **44,** 1353–1359.

SCHMIDT, Z., DOTY, D. R. & DUTTA-ROY, K. 1985 Severe slugging in offshore pipeline riser–pipe systems. *SPE J.* 27–38.

TAITEL, Y., SHOHAM, O. & BRILL, J. P. 1989 Simplified transient solution and simulation of two-phase flow in pipelines. *Chem. Engng Sci* **44,** 1353–1359.

TAITEL, Y., VIERKANDT, S., SHOHAM, O. & BRILL. J. P. 1990a Severe slugging in a riser system, experimental and modelling. *Int. J. Multiphase Flow* **16,** 57–68.

TAITEL, Y., SHOHAM, O. & BRILL, J. P. 1990b Transient two-phase flow in low velocity hilly terrain pipelines. *Int. J. Multiphase Flow* **16,** 69–77.

THERON, B. 1989 Ecoulements diphasiques instationnaires en conduite horizontale. Thèse de docteur-ingénieur, Institut National Polytechnique de Toulouse, France.